

# Phase Field Modeling of Dislocation Network Coarsening, Dislocation – Impurity and Dislocation – Precipitate Interactions

C. Shen, A. Kazaryan, P. M. Anderson and Y. Wang  
Department of Materials Science and Engineering  
The Ohio State University  
2041 College Road, Columbus, OH43210

Interactions of dislocations with one another and their interactions with impurities and precipitates determine the behavior of plastic deformation of crystalline materials. In this presentation, we will discuss recent advances in phase field modeling of dislocation network coarsening, solute segregation and phase transition at dislocations, and migration of dislocations through  $\gamma$  channels in single crystal cuboidal  $\gamma/\gamma'$  microstructures and  $\gamma/\gamma'$  multilayer thin films of superalloys.

## Phase field method

The phase field method was used primarily as a technique for modeling complex microstructural patterns on mesoscopic length scales generated by various phase transformations and grain growth. Comprehensive reviews of the method and its applications can be found in several publications [1-4]. Like other conventional treatments, the method describes microstructural evolution by partial differential equations. However, instead of tracking individual interfacial boundaries, this method describes an arbitrary microstructure as a whole by using a set of mesoscopic field variables that are spatially continuous and time-dependent. The most familiar examples of field variables are the concentration field, which characterizes composition variation, and the long-range order (lro) parameter fields, which characterize structural heterogeneity. The spatiotemporal evolution of these fields can be obtained by solving the semi-phenomenological dynamic equations of motion. Examples are the generalized nonlinear Cahn-Hilliard diffusion equations for the concentration fields and the time-dependent Ginzburg-Landau equation for the lro parameter fields. When including the Langevin noise terms, these equations can describe thermal fluctuations in composition and lro parameters and hence can simulate nucleation phenomena.

The recent development of phase field approach to dislocation dynamics [5] has provided a potential way to model efficiently the motion of large ensembles of dislocations. In this approach dislocations are treated as a set of coherent misfitting martensitic platelets whose stress-free transformation strain (SFTS) is an invariant plane strain given by  $\epsilon_{ij} = (1/2)(b_i n_j + b_j n_i)/d$ , where  $\mathbf{b}$  and  $\mathbf{n}$  are the slip direction (Burgers vector) and slip plane normal, respectively, which are equivalent to the shear direction and invariant plane normal of the martensitic plates, and  $d$  is the inter-planar distance of the slip planes which is equivalent to the thickness of the martensitic plates (Fig. 1). By introducing a new set of order parameters in the field equations to characterize the density of dislocations of a particular elementary Burgers vector on a particular slip plane (each individual order parameter can be interpreted as the disregistry in Peierls-Nabarro theory [6]), the total SFTS field associated with the dislocations can be written in a similar form as the SFTS

field for martensitic precipitates. Substituting this SFTS field into the elastic energy equations formulated for martensitic transformations [7], one obtains the elastic energy of the dislocations. This method has been demonstrated to be very efficient for simulating dislocation dynamics and dislocation-precipitate interactions, and can effectively treat multiplication and annihilation between large numbers of dislocations [5].

### **Dislocation network coarsening**

The coarsening behavior of dislocation networks (substructures) is critical for the understanding of recovery processes. Since the phase field approach does not require tracking individual dislocation lines, it has the potential ability to handle self-consistently any topological changes during dynamic evolution of arbitrary three-dimensional dislocation networks, which is difficult to treat using boundary tracking approaches. The current phase field method is, however, formulated for glide of perfect dislocations on  $\{111\}$  planes in f.c.c. crystals. It does not account for dislocation reactions such as  $1/2[110] + 1/2[\bar{1}0\bar{1}] = 1/2[01\bar{1}]$  which is essential for the understanding of dislocation network formation and coarsening.

In this work we have extended the phase field approach to allow for dislocation reaction and node formation, in accord with Frank's rule. An example of dislocation interaction and relaxation is shown in Fig. 2. Using this model, we have studied the coarsening behavior of complex networks of this type. The simulation results obtained for dislocation network consisting of  $1/2\langle 110 \rangle$  perfect dislocations in an f.c.c. crystal are shown in Fig. 3 and Fig. 4 for two different network configurations. Their coarsening behavior seems to be very different because of the different topological constraints. The work is now being extended to interactions with impurity atoms and forest dislocations. The coarsening behavior of a dislocation network will be discussed in contrast to grain growth where the topological constraints and long-range elastic interactions unique to dislocation networks are absent.

### **Impurity segregation and phase transition at dislocations**

Impurity segregation at dislocations was studied for an edge dislocation using a regular solution model. A first-order transition from low to high solute segregation was predicted for alloy compositions and temperatures that are located outside the two-phase field in the phase diagram (Fig. 5). The effects of such a phase transition on dislocation migration and the Portevin-LeChatelier effect will be discussed.

### **Dislocations migration through $\gamma$ channels in superalloys**

Kinetics of  $\gamma$ -channel filling of dislocations during plastic deformation in single crystal cuboidal  $\gamma/\gamma'$  microstructures and  $\gamma/\gamma'$  multilayer thin films of Ni-based superalloys was characterized as a function of channel width and lattice mismatch between the  $\gamma$  and  $\gamma'$  phases. When the lattice mismatch vanishes, the critical shear stress for a dislocation loop to expand in the  $\gamma$  channel was found to be proportional to  $\ln(s)/s$  where  $s$  is the channel width (Fig.6). For the cuboidal  $\gamma/\gamma'$  microstructures (Fig. 7), it was found that a

dislocation migrating in the horizontal channel driven by an applied shear stress entered into both  $60^\circ$   $\gamma$  channels with equal velocity (Fig. 7(a)) when the lattice mismatch is zero. When the lattice mismatch is finite, however, the dislocation can enter into only one channel under the same applied stress (Fig. 7(b)).

In the study of threading dislocation propagation in multilayers, it was found that the deformation behavior of the film change from confined layer slip in individual layers at large lattice mismatch (Fig. 8(a)) to co-deformation across layers at smaller lattice mismatch (Fig. 8(b)). These results agree well with the predictions made by Anderson et. al. [8] using a newly developed discrete model.

#### References:

1. J. D. Gunton, M. S. Miguel and P. S. Sahni. The dynamics of first-order phase transitions. Phase Transitions and Critical Phenomena, Vol. 8. C. Domb and J. L. Lebowitz, eds (Academic Press, New York, 1983) pp 267-466.
2. Y. Wang, L. Q. Chen and A. G. Khachaturyan. Computer simulation of microstructure evolution in coherent solids. Solid  $\rightarrow$  Solid phase Transformations, eds. W. C. Johnson, J. M. Howe, D. E. Laughlin and W. A. Sofka, (TMS, Warrendale, PA, 1994) pp. 245-265.
3. L. Q. Chen and Y. Wang. 1996. The continuum field approach to modeling microstructural evolution. *JOM*, **48**, pp13-18, Dec. 1996.
4. Y. Wang and L. Q. Chen, "Simulation of Microstructural Evolution Using the Phase Field Method," in Methods in Materials Research, a current protocols publication by John Wiley & Sons, Inc. 2000, pp. 2a.3.1 – 2a.3.23.
5. Y. U. Wang, Y. M. Jin, A. M. Cuitino and A. G. Khachaturyan, "Nanoscale Phase Field Microelasticity Theory of Dislocations: Model and 3D Simulations," *Acta mater* 49 (2001) 1847-1857.
6. F. R. N. Nabarro, "Theory of crystal dislocations", Dover publications, INC. New York, 1987.
7. Y. Wang and A. G. Khachaturyan, "Three-Dimensional Field Model and Computer Modeling of Martensitic Transformations." *Acta Metall. Mater* , **45** (1997) 759.
8. P.M. Anderson, Y. Wang, C. Shen, and Q. Li, "Deformation in Multilayered Thin Films: Phase Field and Discrete Dislocation Modeling", MRS Fall 2001 Symp. "Thin Films: Stresses and Mechanical Properties IX". Boston, MA (Nov. 26-30, 2001).

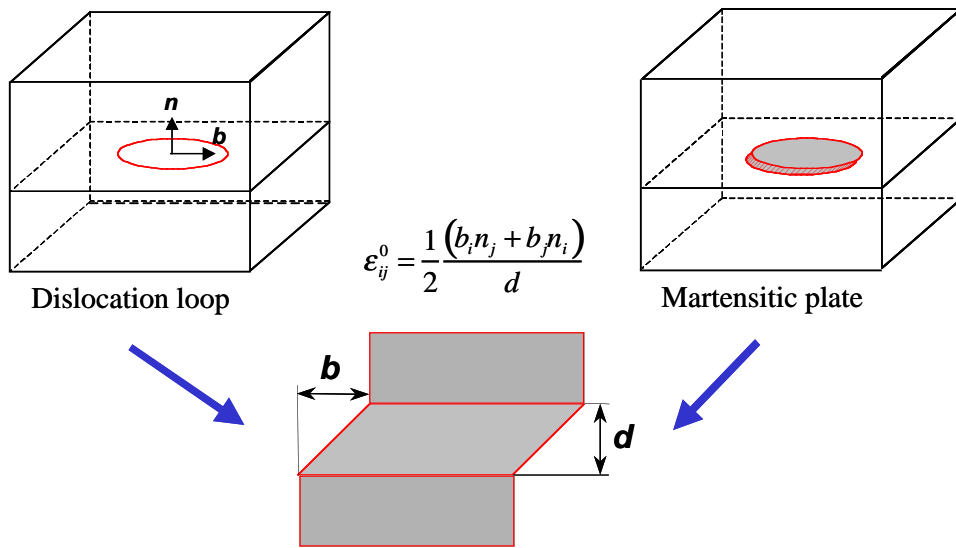


Fig. 1. Phase-field description of dislocations, analogy between a dislocation loop and a martensitic plate.

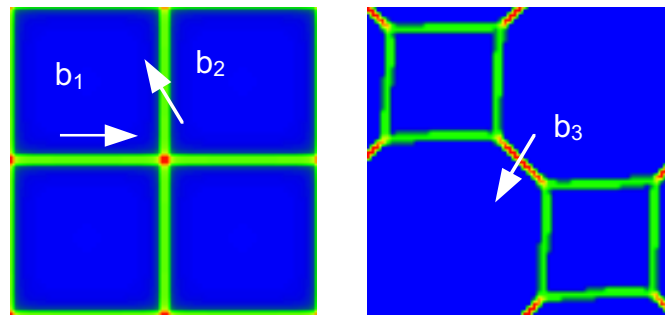


Fig. 2. Phase field modeling of dislocation reaction and network relaxation on a (111) plane. The two initially intercepted dislocation lines (green) with Burgers vectors  $\mathbf{b}_1$  and  $\mathbf{b}_2$  respectively evolve into a new configuration consisting of a new segment with  $\mathbf{b}_3$ , where  $\mathbf{b}_1$ ,  $\mathbf{b}_2$  and  $\mathbf{b}_3$  are three primary Burgers vectors on the (111) plane. Periodic boundary condition is used.

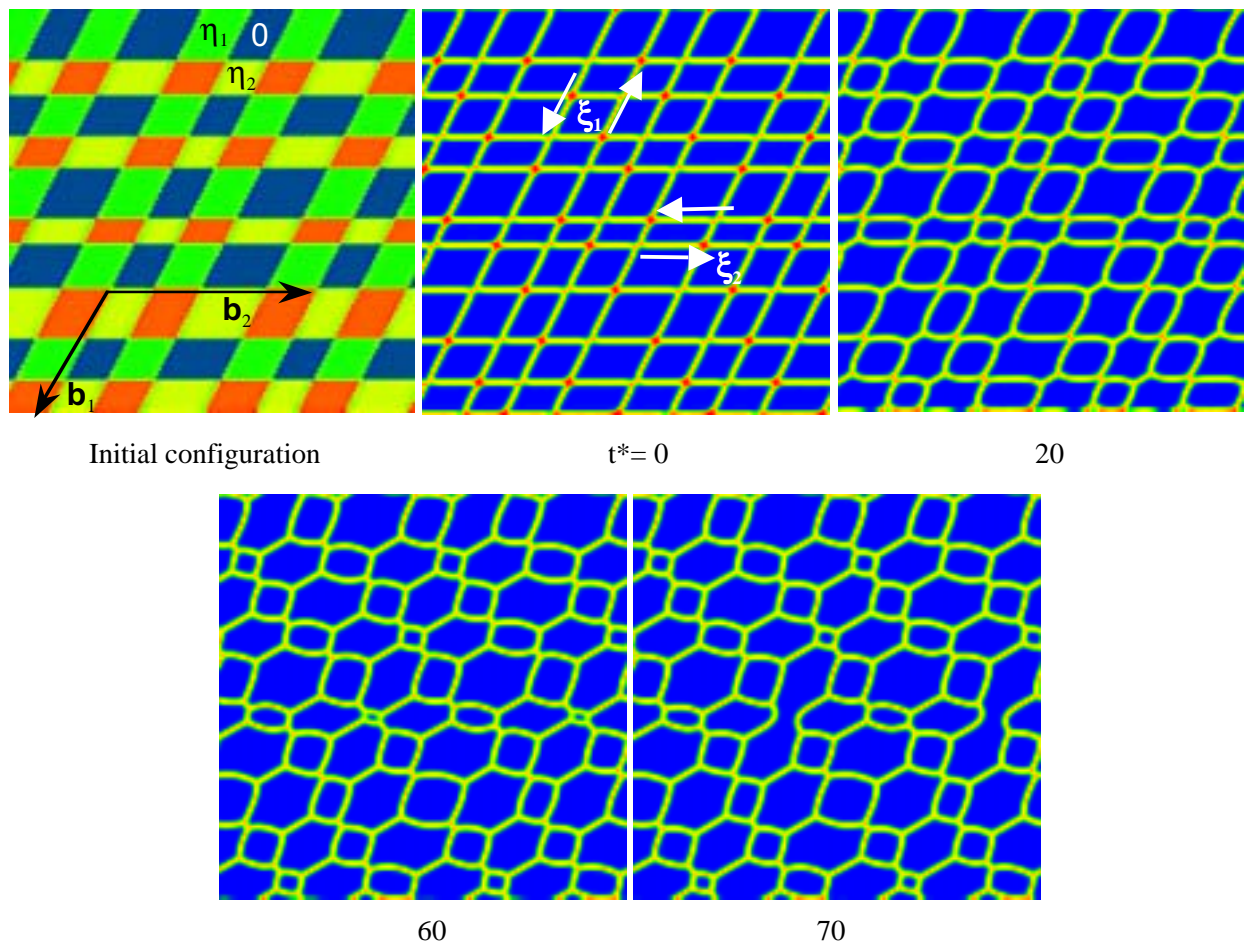


Fig. 3. Evolution of a dislocation network on (111) plane consisting of two types of dislocations loops of  $\mathbf{b}_1$  and  $\mathbf{b}_2$ . The time shown is in reduced unit.

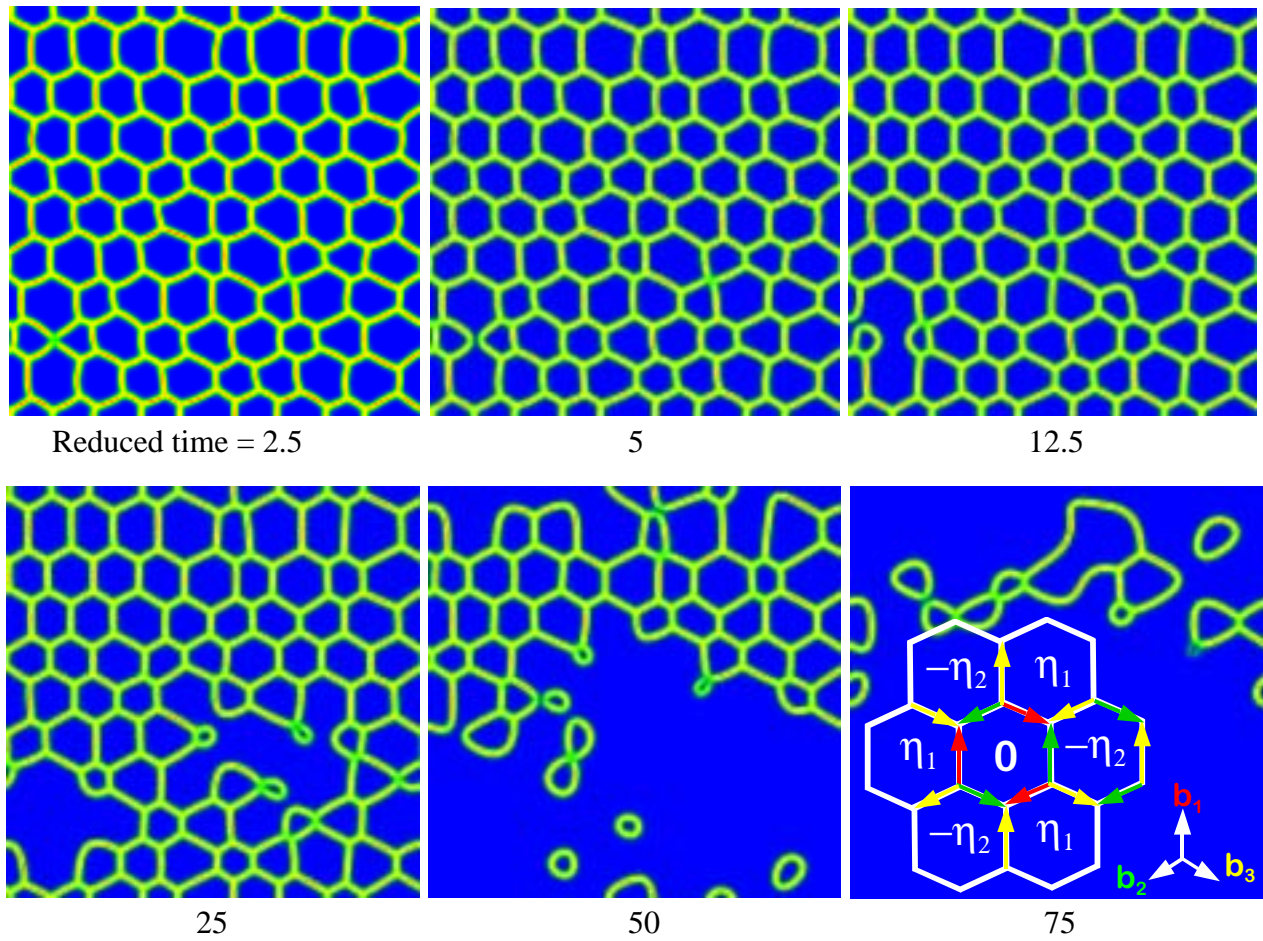
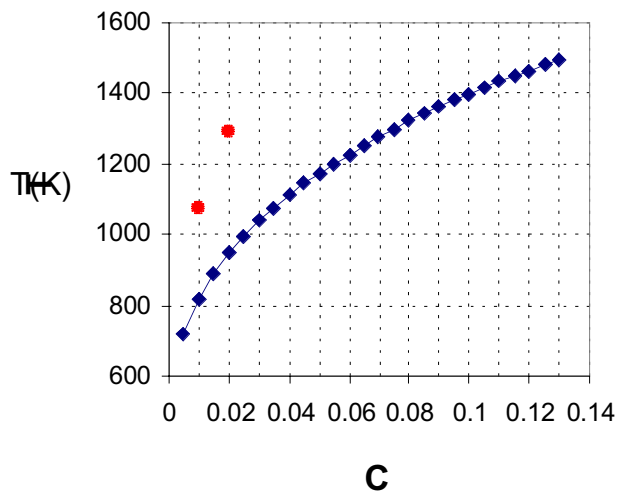
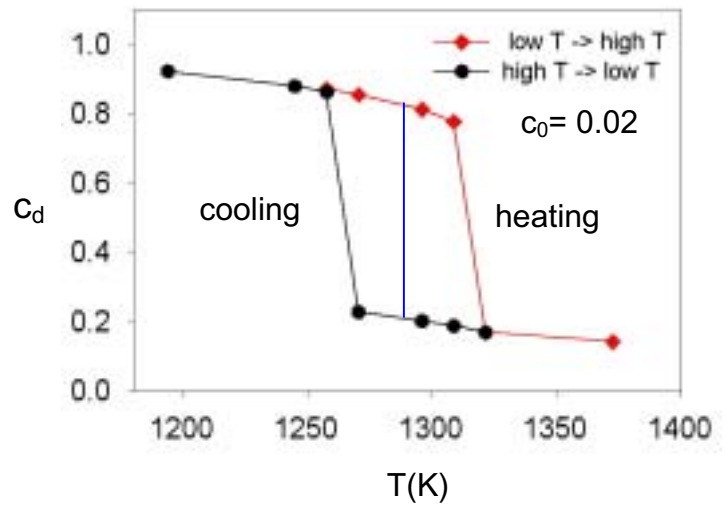


Fig. 4. Time evolution of a dislocation network on (111) plane consisting of three types of dislocations loops of  $\mathbf{b}_1$ ,  $\mathbf{b}_2$  and  $\mathbf{b}_3$ . The sense vectors of the same color have the same Burgers vectors.



(a)



(b)

Fig. 5. (a) Miscibility gap of a binary alloy. The phase transition temperature at dislocation predicted in (b) is indicated by a solid circle. (b) Temperature dependence of solute concentration at dislocation during heating and cooling cycle in a binary alloy of bulk composition of 0.02.

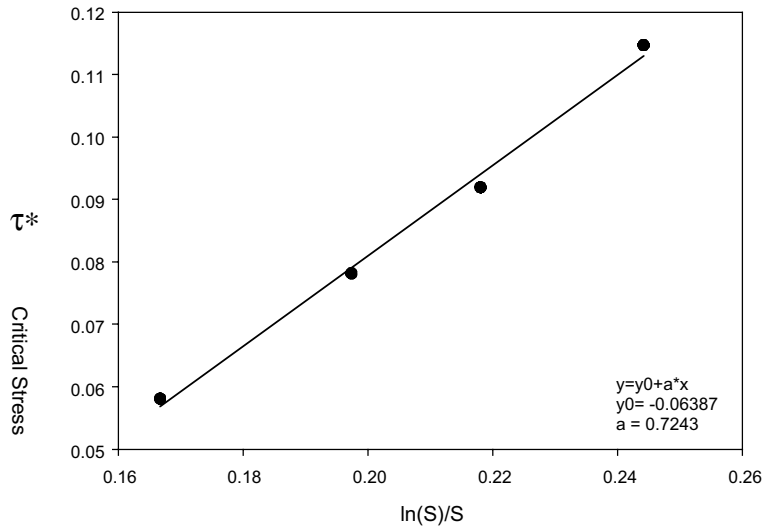
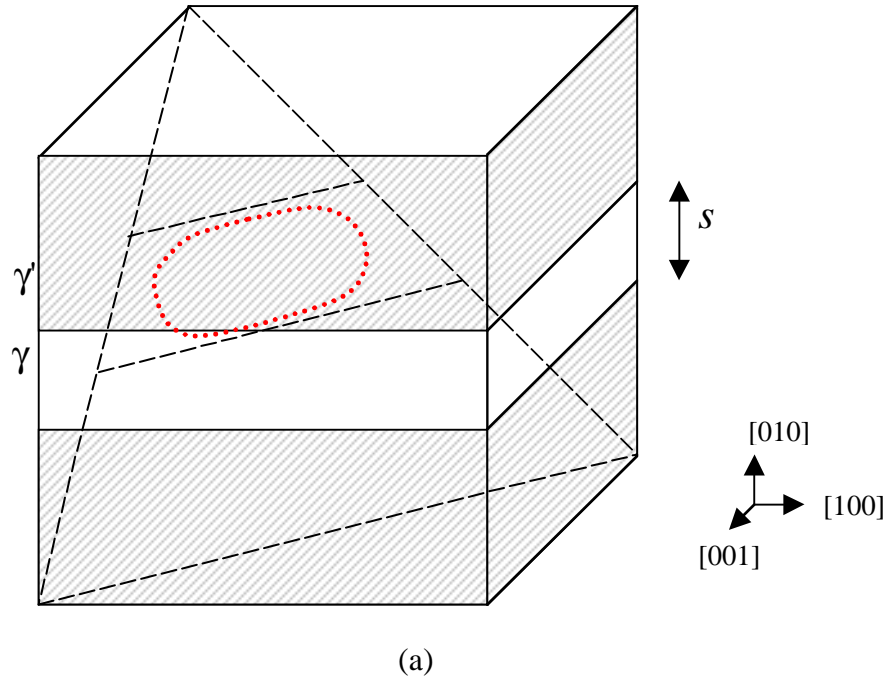


Fig. 6. (a) Schematic diagram showing the geometry used in the simulation. The dotted line is the dislocation loop that is confined in a  $\gamma$  layer. (b) Simulation result of the  $\ln s/s$  dependence of the critical resolved stress  $\tau^*$  (in reduced unit) that drives the dislocation loop through the  $\gamma$  layer, where  $s$  is the width of the layer (in reduced unit).

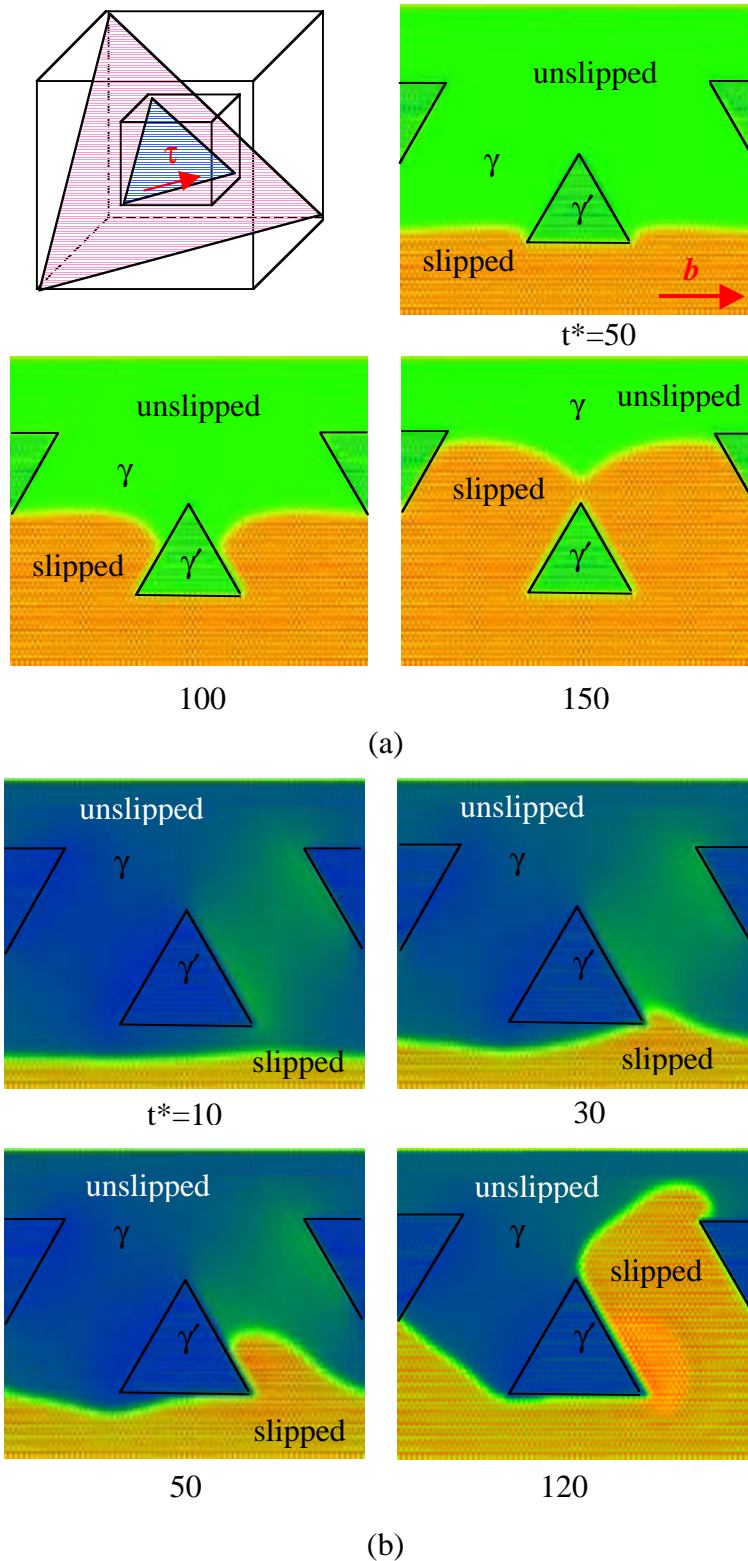


Fig. 7. A  $1/2\langle 110 \rangle$  type screw dislocation enters  $\gamma$  channels in a cuboidal  $\gamma/\gamma'$  microstructure. The two segments in the left and the right channels appear symmetrical in (a) where no  $\gamma/\gamma'$  misfit is considered. It becomes non-symmetrical in (b) due to the presence of the misfit stress.

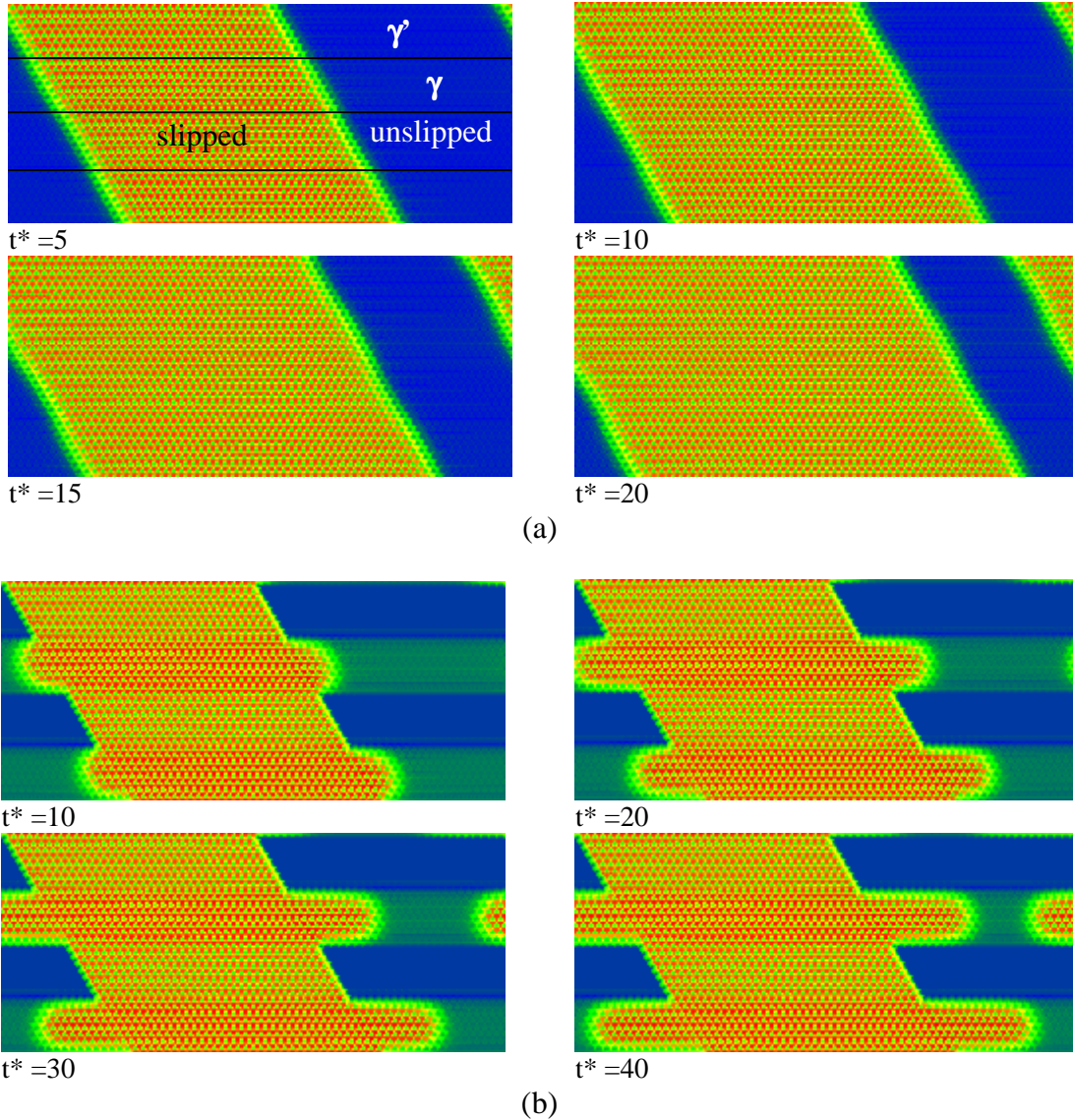


Fig. 8. Phase field modeling of threading dislocations propagation in multilayer  $\gamma/\gamma'$  thin film. (a) Co-deformation across layers at small lattice mismatch and (b) confined layer slip at larger lattice mismatch.  $t^*$  is the reduced time. The crystalline energies of the  $\gamma$  and  $\gamma'$  phases are assumed the same in these simulations, which is different from the simulations shown in Fig. 7 where a higher crystalline energy is assumed for the  $\gamma'$  phase and hence the dislocations cannot cut through the  $\gamma'$  phase.